

Connecting land use–land cover and precipitation with organic matter biogeochemistry in a tropical river–estuary system of western peninsular India

U.K. Pradhan ^{a*}, Y. Wu ^b, P.V. Shirodkar ^c, H.Shiva Kumar ^d and J. Zhang ^b

^{a*} CSIR–National Institute of Oceanography, Regional Centre, Mumbai 400053, India

^b State Key Laboratory of Estuarine and Coastal Research, East China Normal University, 3663 North Zhongshan Road, 200062 Shanghai, PR China

^c CSIR–National Institute of Oceanography, Dona Paula, 403004 Goa, India

^d Indian National Centre for Ocean Information Services (INCOIS), Ocean Valley, Pragathi Nagar (BO), Nizampet (SO), Hyderabad, 500090, Andhra Pradesh, India

*Corresponding author

Abstract

Organic matter (OM) composition changed due to land use– land cover (LULC) and hydrology modification, has distinctive linkage towards sustainable environment management in tropical river systems. It is crucial in small river systems, which experience delay of freshwater flow to the estuaries due to headwater damming, also LULC alteration along the entire basin. In order to understand this fundamental linkage in tropical Zuari river-estuary (ZRE), we analyzed multi-proxy data of organic carbon to total nitrogen ratio (C_{org}/N), stable organic carbon isotope ($\delta^{13}C_{org}$) and lignin phenols measured in seasonally collected suspended particulate matter (SPM) and sediment samples. Results highlighted about moderate seasonality of OM tracers, with a significant effect of LULC alteration, which nevertheless a striking feature in monsoon-fed river-estuaries of peninsular India. Particulate C_{org} export from ZRE estimated to be $20 \times 10^3 \text{ kg yr}^{-1}$, was much lower as compared to tropical river-estuary systems elsewhere. OM fraction from vascular plant (mangroves) contributed to SPM and sediment was 15% and 40%, respectively, calculated using a Bayesian mixing calculation through Stable isotope analysis in R (SIAR). Presence of mudflat LULC in the estuarine region notably caused 20% decrease in C_{org} and 60% increase in lignin phenol (δ^8) as compared to their limits in upstream. This is although mudflat accounts only 3% of ZRE catchment. The degree of shifts in OM tracers highlights towards efficient entrapment, transformation and/or utilization of riverine OM in the mudflats of ZRE. Accelerated human induced LULC dampens the seasonality of OM characteristics and flow is highlighted through this study, which is essential towards sustainable environmental management practice in small rivers of India and World.

Keywords: Particulate organic matter; sedimentary organic matter; Zuari river estuary; carbon isotope; lignin phenols; western peninsular India

1. Introduction

Small Mountainous River-Estuary systems (SMREs) in tropics, generally characterized by high runoff and warmer temperature contribute to significant fraction of global sediment and carbon delivery into the oceans. Globally, SMREs ($\leq 10,000 \text{ km}^2$) contribute to upward of 35% of total terrigenous sediment and particulate organic carbon (POC) supply into the ocean (Milliman and Syvitski, 1992; Lyons et al., 2002). Mineralization and efficient burial of river delivered POC within continental margins plays important role in long-term geochemical cycling of carbon as well as in oceanic biogeochemical cycles (Bolton et al., 2006). In spite of these significance, observations and data on SMREs are sparse in regional as well as global scales, which affect the understanding of organic matter (OM) fluxes, mainly established through extrapolation or modeling (Gomez et al., 2003; Lloret et al., 2013; Hilton et al., 2015).

The linkage between land use/land cover (LULC) and OM composition along the dispersal pathway of SMREs can highlight the interim changes that hamper composition and transport processes of OM. Both LULC and hydrology (dam construction, deforestation, intensive growth in agriculture and population etc.) modification have enormously affected the timing, magnitude and composition of OM in tropical SMRE (Hilton et al., 2010; Wohl et al., 2012; Zhang et al., 2013). Yet, such linkage studies are sparse in tropical SMREs, specifically, in the SMRE networks of south and south-east (SE) Asia. The SMREs of south and south-east Asia collectively deliver $25 \times 10^{12} \text{ m}^3 \text{ y}^{-1}$ volume of freshwater, $8.96 \times 10^9 \text{ t y}^{-1}$ sediment and $0.13 \times 10^9 \text{ t y}^{-1}$ POC, which are equivalent to 70% and 50% and 70% of global freshwater, sediment and POC loads from river to the ocean respectively (Milliman et al., 1999; Huang et al., 2012). Nearly 30,000 large dams, operated in the tropical river systems fulfill water and energy crisis of almost half of the global population (3.6 billion people). Alternatively, they cause significant change in the amount of fluvial load discharge to contemporary seas (World Resources Institute, 2005). Studies have summarized about leveraging fingerprinting of precipitation and LULC change on OM composition as well as flow through tropical SMREs in SE Asia (e.g. Jennerjahn et al., 2004, 2008; Moyer et al., 2013; Wu et al., 2013; Pradhan et al., 2014; Sarma et al., 2014). Results based on limited number of investigations highlighted that OM composition in tropical SMREs, notably follow a dry-wet pattern. They mainly sourced from agriculture soil and plant debris during wet period, whereas from algal detritus during dry period (Wu et al., 2013; Jennerjahn et al., 2004; Pradhan et al., 2016). Dam construction in the headwaters significantly regulates the water flow, causing major fraction of river borne OM to be trapped in the estuarine environment (Sarkar et al., 2016). Exception to this pattern occurs during extreme hydrologic events such as typhoons and flood (Wu et al., 2013; Pradhan et al., 2016). More

than one hundred SMREs are located in the tropical peninsular India. The timing and magnitude of freshwater and sediment discharge from these SMREs frequently changes due to the change in timing of southwest monsoon (SWM) precipitation as well as damming in headwater (Panda et al., 2011; SatyaPrakash et al., 2013). The dam construction albeit supports better sustenance of growing population, but have caused alteration in natural biogeochemistry and ecological processes within the SMRE systems and in nearby seas (Arabian Sea and Bay of Bengal), which nonetheless requires adequate scientific attention. In this study, we report about changing composition of OM with respect to LULC and hydrology in Zuari River–Estuary (ZRE) along the western peninsular India. Elemental, isotopic and molecular geochemical tracer data on SPM and sediment samples were analysed with broad scientific objectives (i) to ascertain the imprints of hydrology and LULC on spatial and seasonal OM loading and (ii) to determine controlling factor of OM composition in ZRE. The use of lignin phenols along with carbon isotope ($\delta^{13}\text{C}_{\text{org}}$) as tracer for OM characterization, is new-fangled to this system, but have previously adopted in studies elsewhere (e.g. Hedges et al., 1984; Goñi et al., 2003). The unique importance of this study across the Indian continental margin and tropical regions of world is that in this study, delineation of natural vs. anthropogenic modification of OM transported through a SMRE is analyzed in the context of global environmental changing practices such as LULC and hydrology modification. Furthermore, the snapshot changes due to above modifications are highlighted, which are more crucial in SMREs as compared to the large systems.

2. Materials and methods

2.1 Study area description

Goa is smallest state in India (area: 3702 km²), with its coastline stretching over 130 km along the Arabian Sea in west and flanked by the Western Ghats in east (Figure 1). Two districts namely North Goa and South Goa covers 46% and 53% of the total area of Goa, respectively. About 90% of the total annual precipitation of Goa occurred during SWM (i.e. from June to September), which fed the river-estuary systems debouching into Arabian Sea (Nandargi et al., 2014). The investigated ZRE is the longest river system (92 km) located in South Goa. The average precipitation over South Goa for the period 2001–2012 was 3150 mm yr⁻¹, which is higher than the long-term average rainfall (3006 mm yr⁻¹: period 1901–2000) for same region (Nandargi et al., 2014). Mean monthly rainfall during September 2011 was 438 mm, which is equivalent to 12% of the total annual rainfall, also higher than the historical (1901–2000) average (Figure 2).

The ZRE is a fifth order stream, with catchment area 973 km² flowing into Arabian Sea through Mormugaobay (Figure 1). The upper ZRE cascaded within a network of three tributaries: Kushavati, Uguem and Guloli, amongst Kushavati joins ZRE at a distance about 40 km from the estuary, whereas Uguem and Guloli join in the upstream near Sanguem (Figure 1). The freshwater flow of ZRE refers to combined flow from Kushavati, Uguem and Guloli tributaries, which account to $2.1 \times 10^9 \text{ m}^3 \text{ yr}^{-1}$ in the year 1981–1998 (Water Resources Department, Goa). The Selaulim dam, with $0.25 \times 10^9 \text{ m}^3 \text{ yr}^{-1}$ freshwater storage capacity was constructed during 1975, within area of 209-km² in Guloli River. A funnel shaped bay (width: 5 km and area: 50 km²) in estuarine region of ZRE stimulates salt–water intrusion roughly 40 km upstream with semi-diurnal tides, which together corresponds to strong vertical mixing especially during post and pre–monsoon seasons (Sundar and Shetye, 2005; Sundar et al., 2015).

The LULC such as natural forest and plantation are dominant of riverine regions of ZRE, whereas agriculture, human settlement and mangrove are dominant in channel region, with mainly human settlement LULC in the bay region (Figure 1). The LULC distributions during pre and post dam period are distinctly different. Figure 1 suggests that agriculture LULC have been replaced by plantation and forest in most of the upper reaches, whereas it is replaced with human settlement in the lower reaches. The population density of Goa in 2011 is nearly two times higher (394 inhabitants/km²) as compared to that in 1971 (214 inhabitants/km²). Overall, the population density of the state is higher than the national average (382 inhabitants/km²; National Commission on Population, India). Activities such as mining of mineral ores largely influenced the river–estuary systems of Goa. There was an increase in the mining area of about seven-times in the last five decade. Also, the export of mineral ores increased from $0.4 \times 10^9 \text{ kg yr}^{-1}$ in 1951 to $35 \times 10^9 \text{ kg yr}^{-1}$ in 2009 (Directorate of Mines and Geology, Goa). More than ten large mines are operated within ZRE and generate mine tailings of about $4 \times 10^6 \text{ kg mine}^{-1} \text{ day}^{-1}$, which normally dumped into the water during transportation (Paimpillil and Nair, 2012). The human induced developmental activities have modified the ecosystem health in terms of change in mangrove resources and estuarine morphology in most of the Goan river-estuary systems (Ramaiah et al., 2007).

2.2 Sampling and pretreatment

To study the OM composition in suspended particulate matter (SPM) and sediment over a space–time scale in ZRE, water samples from 0.5m depth and near bottom sediments were collected along the salinity gradient in riverine (Z1–Z2), channel (Z3) and bay (Z4–Z6) regions during SWM (September), post–monsoon (November) and pre–monsoon (April) seasons of 2011-12 (Figure 1). About 25 L water collected at each location, during neap tide (tidal height: 1–1.5m) were stored in

acid cleaned jars. Samples in the river and channel were collected using a bucket lowered from bridge to the middle of watercourse, whereas estuarine samples collected using 5L Niskin sampler operated from a boat. Salinity and pH were measured right away by using a multi-parameter probe (Inolab multi-720), with analytical precisions ± 0.01 practical salinity unit (psu) and ± 0.001 pH unit, respectively. Samples for chlorophyll *a* (Chl*a*) was filtered through glass micro fiber filters (GF/F: 0.45 μ m), then the filters were drenched overnight in 90% acetone and absorbance of extracted pigments were measured using a UV-Visible spectrophotometer (Lorenzen, 1967). SPM were collected by filtering known volume of water through pre-weighed 47 mm GF/F filters (pre-combusted at 450°C for 5 hr), later the filters were used for elemental and isotopic measurement. For lignin phenol, 10–15L of water filtered through 142 mm GF/F filters (0.45 μ m) using a N₂ pressure filtration system, then the filter was oven-dried at 45°C.

OM end-members such as leaves and woods of dominant mangrove (*K. candel*, *S. alba*, *A. officinalis*, *R. mucronata*, *S. Caseolaris*) and terrestrial plants were picked from their litters. Flowers (*Calendula Officinalis*, *chrysanthemum*, *Rose*) were collected from floral wastes dumped into the river. Soil samples affected by termite and mining dust in the headwater region were collected in this study. Sediments collected using avan-veen grab were stored at 4°C. Sediments, soils and plant organs were oven-dried at 45°C and homogeneously pulverized prior to the chemical analyses.

2.3 Rainfall, hydrology and LULC

Mean monthly rainfall data was obtained from Indian Meteorological Department (www.imd.gov.in) and freshwater discharge data was obtained from Goa State Water Resource Department. Landsat TM (Thematic Mapper) images for December 1976 and December 2015 were used with pixel resolutions 60m and 30m, respectively. The images were acquired from USGS land cover facility (<http://earthexplorer.usgs.gov/>) through Landsat-2 and Landsat-8. Supervised image classification toolbar was used with 85% target accuracy in the classification (Anderson et al., 1979). Digital Elevation Model (DEM) data used for the drainage network delineation (30 m resolution) through ASTER and <http://gdem.ersdac.jspacesystems.or.jp/search.jsp>. The LULC categories are expressed as cultivable land, settlement with mixed crop, forest with mixed plantation, mangroves, mining, mudflats, open scrubland and water bodies. ERDAS Imagine (2015) and Arc Map 10.3.1 are used to determine the composition of LULC. The LULC categories further partitioned at 5 × 5km boxes along the freshwater-tidal portion of ZRE and used for statistical comparison.

2.4 Chemical analyses

Contents of organic carbon and total nitrogen in SPM are abbreviated as POC and PN respectively, whereas the same in rest of samples (plant organs, soil and sediments) are abbreviated as C_{org} and TN, respectively. $\delta^{13}C_{POC}$ refers to stable carbon isotopic ratio in SPM, whereas $\delta^{13}C_{org}$ refers to stable carbon isotopic ratio in plant organs, soil and sediments. Weight percentages of POC, PN, C_{org} and TN were determined using an Elemental Analyzer (Vario EL III; Elementar Co.). $\delta^{13}C_{POC}$ and $\delta^{13}C_{org}$ were determined using a Flash EA 1112 Elemental Analyzer interfaced with continuous flow Isotope Ratio Mass Spectrometer (DELTA plus/ XP). Prior to the analysis of POC and $\delta^{13}C_{POC}$, inorganic carbon was removed by exposing filters to concentrated hydrochloric acid (HCl) fumes in a desiccator for 24 hr and then dried at 45°C. Similarly, prior to the measurements of C_{org} and $\delta^{13}C_{org}$, soil and sediments (plants have negligible $CaCO_3$) were de-carbonated using HCl acidification (repeated addition of 2–3 drops of purified 6N HCl). Measurement of PN and TN performed directly on untreated samples. Acetanilide used as calibration standard for POC, PN, C_{org} and TN measurement, whereas $\delta^{13}C_{POC}$ and $\delta^{13}C_{org}$ was determined relative to air. Determinations of $^{13}C/^{12}C$ expressed relative to conventional standard Vienna–Pee Dee Belemnite (V–PDB) for carbon (Coplen, 2011), with relative isotope–ratio difference δ defined as:

$$\delta X = [(R_{sample} - R_{standard})/R_{standard}] \times 10^3 \quad (\text{eq. 1})$$

Where $X=^{13}C$, $R =^{13}C/^{12}C$ and δ is expressed in parts per mil with symbol ‰ (Coplen, 2011). Replicate analyses of selected samples (n=10) produced precision (percentage standard deviation) of $\leq 5 \delta$ for POC, PN, C_{org} and TN, and standard deviations of $\leq 0.1 \delta$ for $\delta^{13}C_{POC}$ and $\delta^{13}C_{org}$.

Grain size measurement of sediment samples were performed using a Coulter laser granular meter (LS–100Q) after treatment with, $10 \delta H_2O_2$. The sediment grain sizes are expressed as proportion of clay ($<4 \delta m$), silt ($4–63 \delta m$) and sand ($>63 \delta m$), with a measurement error of $\leq 1 \delta$ in the entire dataset.

2.5 Lignin phenols

Lignin phenol was measured as per the method of Goñi and Montgomery (2000), involved gas chromatographic separation along with flame–ionization detection of phenols released through alkaline copper (II) oxide oxidation and later quantified relative to internal standards added during extraction. Briefly, 50–500 mg of powdered samples so as to have at least 5 mg POC or C_{org} were oxidized using CuO and $2 \text{ molL}^{-1} NaOH$ in sealed Teflon vessel and under positive N_2 pressure. The digestion was performed in a Microwave Accelerated Reaction System (MARS5; CEM) at 150°C for

90 minutes at 55-70 PSI pressure. A known amount of Ethylvanillin was added into the digested samples in order to check the analytical recovery. Recovery rate of Ethylvanillin was 95±2% during this study. The phenolic monomers were analyzed as trimethylsilyl derivatives of N,O-bis(trimethylsilyl)trifluoroacetamide (BSTFA) and trimethylchlorosilane (TMCS) (99:1) using a Agilent 6890N gas chromatography as replicated from Yu et al. (2011) and Pradhan et al. (2014), and closely concur with Goñi and Montgomery (2000). The mean relative precisions for different CuO products calculated by repetitive measurement of a specific sample and found to be ≤10% in this study.

Lignin oxidation products, $\Sigma 8$ (normalized to dry mass of SPM or sediment) and $\Sigma 8$ (normalized to the contents of POC or C_{org}) are defined as sum of VP (vanillyl phenols) = (vanillin; V1 + acetovanillon + vanillic acid; Vd), SP (syringylphenols) = (syringaldehyde; S1 + acetosyringone; Sn + syringic acid; Sd) and CP (cinnamyl phenols) = (p-coumaric acid; PCD + ferulic acid; FAD). Both refer to total plant-derived OM in samples. Angiosperm (flowering) plants have abundant SP, whereas non-woody plants have primarily higher CP. The SP/VP (or S/V) and CP/VP (or C/V) ratios briefly can highlight origin of plant OM in the sample (Hedges et al., 1982; Goni et al., 2003). Similarly, Vd/V1 ratio or (Ad/Al)_{VP} can highlight about the degree of degradation of plant OM in sample such a way that during degradation, relative abundance of acid monomer will increase resulting higher (Ad/Al)_{VP} ratio (≥ 0.5 ; Hedges et al., 1986). This interpretation is not straightforward, because change in the (Ad/Al)_{VP} ratio can be occurred during leaching as well as mineral sorption (Hernes et al., 2007). The contents of SP, VP and CP normalized with $\Sigma 8$ to obtain lignin phenol vegetation index (LPVI), which can avoid misinterpretation regarding degradation of plant OM [Tareq et al. (2004)];

$$LPVI = \left[\frac{S(S+1)}{(V+1)+1} \times \frac{C(C+1)}{(V+1)+1} \right] \quad (\text{eq. 2})$$

The ratios such as P/(V+S) and DHBA/V resulted from non-lignin CuO oxidized products; p-Hydroxyphenols (P) [p-hydroxybenzaldehyde; P1 + p-hydroxyacetophenone; Pn + p-hydroxybenzoic acid; Pd] and benzene carboxylic acid [3,5-dihydroxybenzoic acid; DHBA] and can be used to describe degradation/ humification state of plant OM. Among the p-Hydroxyphenols, Pn is derived from lignin source. Therefore, The Pn/P ratio is also used to highlight relative abundance of non-plant materials in sample (Otto and Simpson, 2005; Houel et al. 2006).

2.6 Statistical analyses and mixing model

Seasonal variation in the geochemical data was checked for statistical significance (95% confidence interval) using one-way ANOVA after Komogorov–Smirnov normality and homogeneity test. The

result of normality test was significant ($p < 0.05$), which highlighted the non-normal nature of data, later normalized through z-scale transformation to avoid variations in data dimensionality (Ross, 1988). Inter-relationships among the parameters were inferred through Pearson's correlation coefficients (r) and regression coefficients (R^2). The primary forcing on OM composition change was evaluated using principal component analysis (PCA) analysis, which used the normalized data of geochemical parameters in SPM along with LULC. Due to the limited sample size, sediment data was not included in PCA. The principal components (PC) having Eigen values >1 exhibit strong influence on data variances, therefore are included (Pradhan et al. 2014). The overall forcing of a particular PC during different seasons was evaluated through an Absolute Principal Component Score (APCS) receptor model. The APCS has advantage of quantifying source contributions mainly characterized through PCA and multivariate analysis of chemical properties (Watson et al., 2002). The chemical properties are distinguished and representative of OM properties. APCS was calculated using following formula:

$$y = \sum B_i X_i + b \quad (\text{eq. 3})$$

Where, ' B_i ' is the regression coefficient, ' X_i ' is component scores (independent variable), ' y ' is parameters used (dependent variable) and ' b ' is the intercept. Influence of independent variable on dependent was evaluated based on regression coefficients. The intercept ' b ' considered as zero, since we used normalized data, therefore equation 3 becomes:

$$y = \sum B_i X_i \quad (\text{eq. 4})$$

On an average, the contribution of a factor ' i ' to the variability in parameter can be calculated as follows;

$$i (\%) = (B_i / \sum B_i) \times 100 \quad (\text{eq. 5})$$

Here, $B_i / \sum B_i$ is the ratios of regression coefficients for factor ' i ' and sum of all regression coefficients.

The provenance of OM was identified from the proximity between limits of elemental and isotopic ratios in major OM pools and the same in SPM and sediment samples. The relative contribution of major OM sources to the SPM and sediment was quantified using a modern Bayesian mixing model SIAR (Stable isotope analysis in R), available in open source R-package (<http://cran.r-project.org/>). One of the advantages of SIAR is that, straightforward way it deals with variability in sources and mixtures with uncertainties (e.g. mean and standard deviation) and thereby estimates the proportional contributions from potential sources. It includes residual error in the form of standard deviations and use Markov Chain Monte Carlo (MCMC) simulation method to produce

potential values of proportional sources within a fitting algorithm (Jackson et al. 2009; Parnell et al. 2010). The covariance structures included in the model provide information on the functional ability and categorize the sources with matrix plots. The matrix plot produces actual correlation coefficients of posterior distributions that represent the correlation between sources in such a way that, if two sources are very close to each other, then most feasible solutions could involve one or other sources but not both at the same time (Parnell et al., 2010). The SIAR has been used previously in studies for quantification of OM proportions in river–estuary and coastal systems (Dubois et al. 2012; Sarma et al. 2014; Krishna et al. 2015; Pradhan et al., 2016). The use of $\delta^{13}\text{C}_{\text{org}}$ and N/C was favorable in the model as $\delta^{13}\text{C}_{\text{org}}$ tends to zero in plankton, which may likely to affect the result. The end-member limits were from this study and adopted from previously available values in the west coast of India. The statistical analyses were performed using SPSS 10.0 (USA Inc.) and results presented using Grapher 4.0 (USA Inc.).

3. Results

3.1 LULC, Precipitation, hydrology and hydrographic parameters

Freshwater discharge in ZRE was dominant from June to September prior to the dam construction. Post-dam (present), freshwater in ZRE delayed by a month (Figure 3a). Lower ZRE receives freshwater mainly from Kushavati tributary during June. From July onwards it receives water from Selaulim dam (discharge: $334 \pm 23 \text{ m}^3\text{s}^{-1}$) as well as Kushavati (discharge: $282 \pm 20 \text{ m}^3\text{s}^{-1}$) (Figure 3b). Freshwater discharge from Selaulim dam was minimal in June. Higher rainfall (compared to the long-term average) over South Goa during September 2011 accelerated the discharge of Kushavati (nearly four times) (Figure 2 and 3). LULC results highlighted that human settlement area increased by ten times ($12 \pm 120 \text{ km}^2$), cultivation area decreased by three times ($292 \pm 113 \text{ km}^2$) and mining increased by six times ($1.2 \pm 7 \text{ km}^2$) between pre and post dam period in ZRE. Also, an increased mangrove and plantation noticed during post-dam period (Table 1; Figure 1). Figure 1 displayed that the proportion of LULCs such as vegetation (cultivation and forest) and human settlement decreased from river towards bay, whereas the proportion of mudflat increased in the channel and bay. Such variability in hydrology and LULC is likely to affect OM biogeochemistry in ZRE.

Distribution of water temperature followed a parabolic trend, with higher values in channel during post and pre-monsoon, showing similar values during SWM along the entire stretch (Table 1). Seasonally, average water temperature was significantly higher during pre-monsoon ($32.1 \pm 0.9^\circ\text{C}$), than post-monsoon ($30.5 \pm 0.9^\circ\text{C}$) and SWM ($28.9 \pm 0.6^\circ\text{C}$). The pH across all sites

was neutral or slightly alkaline, with mean values similar in SWM (7.4 ± 0.7), post-monsoon (7.6 ± 0.6) and pre-monsoon (7.6 ± 0.4). The pH was nearly a unit lower at riverine end (Z1) during SWM owing to discharge of dammed rainwater (Table 1). The salinity ranges were significantly higher during pre-monsoon (0 ± 35 psu, mean 28 ± 9 psu) than post-monsoon (0 ± 34 psu, mean 27 ± 11 psu) and SWM (0 ± 19 psu, mean 15 ± 6 psu). Limits of Chl *a* as fraction of POC averaged at 1.1 ± 0.3 , 0.9 ± 0.5 and 0.8 ± 0.5 mg g⁻¹ POC during SWM, post and pre-monsoon, respectively. Inter-relationship between Chl *a* and salinity was negative in post and pre monsoon, but was positive in SWM indicative towards freshwater biological production (Figure 4).

3.2 Concentration and bulk isotopic properties

The SPM concentrations were ranged at 1.3 ± 33 mgL⁻¹ (av. 13.7 ± 11.7 mgL⁻¹), 11 ± 44.4 mgL⁻¹ (av. 23.7 ± 12.9 mgL⁻¹) and 3.5 ± 165.6 mgL⁻¹ (av. 43.7 ± 68.6 mgL⁻¹) during SWM, post and premonsoon, respectively. SPM increased with salinity fairly in all season, significant during SWM (Figure 4). Higher SPM (44 ± 166 mgL⁻¹) observed in the bay (Z4), was coincided with higher mudflat LULC (~4 km²), lower Chl *a* ($1-6$ mgg⁻¹ POC) and higher POC (0.6 ± 3.4 mgL⁻¹), specifically during post and premonsoon (Figure 5). POC and SPM have scattered relationships with salinity, except that POC showed a significant negative variation with salinity during post-monsoon (Figure 4). POC normalized with SPM was higher in pre-monsoon (1.8 ± 13.4 , mean 6.8 ± 5.6) and SWM (2 ± 38.8 , mean 13.8 ± 15.6), as compared to post-monsoon (1.4 ± 9.4 , mean 3.6 ± 3.2). POC at riverine region (Z1) was 0.52 mgL⁻¹, associated with lower SPM (1.3 mgL⁻¹) during SWM and concurred with highest water discharge from Selaulim dam (Figure 3). POC at the same station during pre-monsoon 0.47 mgL⁻¹ also, aligned with low SPM (3.5 mgL⁻¹). A first-order POC export from ZRE estimated by multiplying average POC (0.5 mgL⁻¹) with annual discharge from Selaulim dam. The POC export from ZRE was 20×10^3 kg yr⁻¹, with a yield of 0.02 g POC m⁻² yr⁻¹ that is much lower than the POC yields from other tropical SMREs such as Wenchuanhe and Wenchanghe in Hainan Island (e.g. Wu et al., 2013). Concentrations of PN showed similar trend as POC and both POC and PN were correlated with each other across all the seasons ($R^2=0.95$; $p<0.001$; figure not shown, Table 1). Average POC/PN ratios were similar throughout this study (SWM 9.0 ± 5.5 ; post-monsoon 9.5 ± 2.0 ; and pre-monsoon 9.1 ± 1.6) and POC/PN ranged from 1.6 to 19.8, with a lowest ratio 1.6 that stands out as outlier, due to higher PN (Table 1). The range of $\delta^{13}C_{POC}$ was from -22.1% to -34.1% (av. $-27.4 \pm 4.9\%$), -20.7% to -29.4% (av. $-24.5 \pm 3.4\%$) and -21.7% to -33.6% (av. $-27.9 \pm 5.2\%$) during SWM, post and pre-monsoon, respectively, increased with salinity, without any marked seasonal shift (Table 1; Figure 4). Longitudinal trends in geochemical parameters were related with aerial featured LULC

(Figure 5). Riverine stations resulted lower $\delta^{13}\text{C}_{\text{POC}}$ that is significantly lower than other values during entire investigation and linked with higher Chl *a* and vegetation LULC (Figure5).

$\delta^{13}\text{C}_{\text{org}}$ of botanical samples indicated dominance of C_3 plants (mangroves) that conceivably act as major source of plant OM mixed through littering in ZRE (Table 2). Soils collected in ZRE exhibited $\delta^{13}\text{C}_{\text{org}}$ range of -21.4‰ to -22.9‰ , typically higher than the plant and bottom sediments (Table 2). $\delta^{13}\text{C}_{\text{org}}$ in sediment samples were ranged from -23.6‰ to -26.5‰ (av. $-25.3 \pm 1.2\text{‰}$). Average $\text{C}_{\text{org}}/\text{N}$ ratio of sediment was higher during pre-monsoon (23.4 ± 26) than post-monsoon (15.8 ± 6.8) and SWM (11.4 ± 1). The grain size compositions of sediment dominantly silt and sand, overall grain sizes were: SWM (clay: $21.8 \pm 8\%$; silt: $43.4 \pm 10.9\%$ and sand: $35.6 \pm 17.1\%$), post-monsoon (clay: $28 \pm 8.9\%$; silt: $50 \pm 4.2\%$ and sand: $22.5 \pm 12.1\%$) and pre-monsoon (clay: $23.9 \pm 20.3\%$; silt: $33.8 \pm 28.8\%$ and sand: $42.9 \pm 48.9\%$). There was a positive relationship between contents of clay and C_{org} during all the seasons.

3.3 Lignin phenols and ratios

Plant litters dominantly mangrove leaves exhibited highest lignin yield ($\delta = 44\text{--}392 \text{ mg } 10\text{g}^{-1} \text{ dw}$) as compared to SPM, soil and sediment (Table 2). The average lignin yield of SPM ($\delta = 2.5 \text{ mg } 10\text{g}^{-1} \text{ dw}$) is nearly three times lower than that in sediment ($\delta = 6.4 \text{ mg } 10\text{g}^{-1} \text{ dw}$) during post and pre-monsoon. In general, the relative abundance of PP and VP were higher in SPM, whereas abundance of VP and SP were higher in sediment (Supplementary Table). Considering average δ as $4.3 \pm 2.5 \text{ mg } 100\text{mg}^{-1} \text{ C}_{\text{org}}$ (obtained for plant litter in ZRE), the estimated average vascular plant derived OM into SPM and sediment were nearly 15% and 70%, respectively. The average limits of δ in SPM were consistent among SWM ($0.5 \pm 0.3 \text{ mg } 100\text{mg}^{-1} \text{ POC}$), post-monsoon ($1.0 \pm 0.6 \text{ mg } 100\text{mg}^{-1} \text{ POC}$) and pre-monsoon ($0.3 \pm 0.1 \text{ mg } 100\text{mg}^{-1} \text{ POC}$). Moreover, the δ of SPM were notably lower than that in sediments during SWM ($3.3 \pm 2.0 \text{ mg } 100\text{mg}^{-1} \text{ C}_{\text{org}}$), post-monsoon ($2.5 \pm 1.8 \text{ mg } 100\text{mg}^{-1} \text{ C}_{\text{org}}$) and pre-monsoon ($2.5 \pm 1.6 \text{ mg } 100\text{mg}^{-1} \text{ C}_{\text{org}}$) as well as in soils and plant tissues (Table 2). The overall pattern of δ distribution in SPM had close resemblance with δ roughly decreased from river to bay during all season, significant during SWM and pre-monsoon (Table 2; Figure 4). The elevated δ noticed in bay (Z4) during post-monsoon coincided with higher mudflat, lower S/V and $(\text{Ad}/\text{Al})_{\text{VP}}$ ratios and associated with fairly similar PP, VP and SP. (Table 2; Figure 5). The relative composition of plant tissues present in SPM and sediment were found to be different in ZRE (Figure 6). SPM and sediment showed different ranges of C/V (SPM: 0.22–0.57; sediment: 0.06–0.26) and S/V ratios (SPM: 0.63–1.25; sediment: 0.34–0.97), without any marked seasonal shifts and fall on a mixing line between woody and non-woody angiosperm tissues (Figure 6). The diagenetic state of plant OM is higher in SPM [$(\text{Ad}/\text{Al})_{\text{VP}} = 0.59\text{--}3.33$] than sediment

[(Ad/Al)_{VP} = 0.26–0.49]. The C/V vs. DHBA/V indicated OM mobilization through surface soil and indicators such as DHBA/V and Pn/P showed statistically significant seasonal differences ($p < 0.05$; Table 1)

The ratio of mudflat and vegetation (mangrove, forest and agriculture) that represent mudflat LULC and the ratio of vegetation and settlement that represent vegetation LULC were related with seasonal means of geochemical parameters (Figure 7). SPM concentrations varied significantly with increased mudflat LULC. Relationships; POC (wt. %) vs. mudflat (km²) and POC vs. vegetation (km²) were opposite to each other and $\delta^{13}\text{C}_{\text{POC}}$ negatively varied with vegetation LULC. $\delta^{13}\text{C}_{\text{POC}}$ exhibited moderately positive relationships with mudflat LULC, whereas $\delta^{13}\text{C}_{\text{POC}}$ varied positively with vegetation LULC (Figure 7). Ratios such as S/V and (Ad/Al)_{VP} decreased with increasing mudflat LULC, without any covariance with vegetation LULC. Similarly, the Pn/P ratio decreased with vegetation LULC. The relationship of LULC with geochemical tracers in sediment was found not significant. The OM tracers exhibited notable shifts within the channel affected by mudflat LULC and thereby change towards bay. Vegetation LULC in channel region was nearly two-times lower than that in riverine region. Overall the change in LULC around channel region significantly correspond to decrease of POC by 20% and Chl *a* by ~50%, whereas it provokes increase of $\delta^{13}\text{C}_{\text{POC}}$ by 80‰ and $\delta^{13}\text{C}_{\text{POC}}$ by ~60‰ during this study.

3.4 Multivariate statistics and OM quantification

PCA analysis described here is based on the criteria that $\delta^{13}\text{C}_{\text{POC}}$ represent unique plant OM, carbon normalized yields of Pl, Pd and DHBA as indicators of non-lignin phenols, land use components such mudflat and vegetation LULC, whereas $\delta^{13}\text{C}_{\text{POC}}$, POC, PN/POC and Chl *a* represents OM quality along with salinity and SPM as supplementary parameters. Positive loading of Chl *a*, POC and vegetation LULC, with negative loading of salinity and $\delta^{13}\text{C}_{\text{POC}}$ in PC1 was indicative towards autochthonous/ biological production. The non-lignin products in PC2, mainly originated from algae or other biological sources with close proximal to lignin products ($\delta^{13}\text{C}_{\text{POC}}$, Pn, DHBA) mainly indicate allochthonous OM and depicted in PC3 with mudflat LULC (Figure 8). Therefore, the PC3 can be termed as physical mixing. The seasonality in the impact of these two factors on overall OM characteristics was obtained from an APCS receptor model. The impacts of biological production and mixing on the OM compositions are 51% and 49% respectively nearly equal during SWM. The impact of allochthonous OM mixing was higher (98%) during post-monsoon, whereas impact of autochthonous OM production was higher (97%) during pre-monsoon season. Multiple OM sources constrained with the help of isotopic, elemental ratio and biomarker limits were clustered with those of SPM and sediments in ZRE (Figure 9). The end member

compositions adopted were previously reported along west coast of India. Broadly, the OM from major sources such as mangrove plant, soils and plankton (freshwater and marine) significantly contributed to SPM and sediment OM compositions. The median value of OM contribution obtained from SIAR model is discussed here. OM contributed from freshwater plankton to SPM was 35% and 30% during SWM and pre-monsoon respectively. OM from soil (30%) and estuarine plankton (33%) into SPM were dominant in post-monsoon. The contribution of OM from sources such as soil and vascular plant (mangrove) to the sediments of ZRE was ~40% during SWM as well as post-monsoon (Figure 9).

4. Discussion

LULC change, dam-controlled hydrology and estuarine physical process have caused exchange of SPM, with disproportionately composed OM in substantial quantity along the ZRE (Figure 2 and 3). Climatologically, ZRE receives runoff through precipitation during SWM and experience hot-humid weather during pre and post monsoon. The dam releases water roughly after one month during SWM. Seasonally contrast climatic feature significantly reflected through variations of water temperature and salinity during the study, also similar in most Indian estuaries (Reddy and Rao, 1994). Consistent variation of *Chla* with salinity was relative to autochthonous biological production, which was significant during pre and postmonsoon, nevertheless hindered by the effect of hydrology during SWM.

4.1 Biogeochemistry of OM in ZRE

The watershed runoff and lateral transfer of SPM from mudflats correspond to seaward increase of SPM during all the seasons (Figure 4). Seaward increase of SPM also can be influenced by estuarine turbidity maximum (ETM) that characteristically occur in ZRE owing to tidal and wind-induced current movement (Rao et al., 2011). The highest freshwater discharge record in ZRE during SWM ($130 \text{ m}^3 \text{ s}^{-1}$) was low, as compared to discharge limits of other tropical SMREs (e.g. Jennerjahn et al., 2004, 2008; Wu et al. 2013; Pradhan et al., 2016). Nevertheless, occasional individual rain events can contribute to major part of their annual water fluxes in tropical SMREs (e.g. Kao and Milliman, 2008). In addition to runoff and ETM, which explained proportional SPM variation in ZRE, lateral transfer of SPM by mudflat LULC could be an important factor as indicated by linear relationship of SPM with mudflat LULC (Figure 5). Also, such LULC effects enhance SPM composition change in ZRE due to assortment process and tiny catchment size. Low SPM high *Chl a* relation observed in ZRE is a characteristic feature of many tropical SMREs [e.g. Wanquanhe; Wu et al. (2013), Mandovi; Khodse and Bhosle (2012) and Wonokromo and Porong; Jennerjahn et al.

(2004)]. Unlike on hydrographic properties, effects of LULC and dam regulated hydrology significantly impinged on seasonality of SPM, Chl *a* and geochemical parameters (POC, PN, $\delta^{13}\text{C}_{\text{POC}}$ and lignin phenols) in ZRE. Processes such as light inhibition on in-situ biological productivity (Bouillon et al., 2009) hampered the salinity vs. POC relationship, which was negative during all the seasons, with higher freshwater biological production during post-monsoon (POC vs. Chl *a*; Pearson's $r = 0.99$). POC varied negatively with SPM and mudflat LULC, whereas positively with vegetation LULC, together suggestive towards presence of organic poor vegetation materials in SPM (Table 1; Figure 5). This could be the vegetative detritus e.g. mangrove leaf litters, flowers etc, which sink faster (8 to 15 weeks) into sediments during pre and post monsoon. The litter yields of dominant mangrove specie *A. officinalis* ($102 \text{ kg km}^{-2} \text{ yr}^{-1}$), *R. mucronata* ($118 \text{ kg km}^{-2} \text{ yr}^{-1}$) and *S. alba* ($170 \text{ kg km}^{-2} \text{ yr}^{-1}$) significantly (80–90%) decompose in river-estuary systems of Goa (Wafar et al., 1997).

Interrelationship between POC and PN (mgL^{-1}) was linear, with a negative intercept on POC ($\text{PN} = 0.9 \times \text{POC} - 0.3$; $R^2 = 0.62$; Figure not shown) during SWM indicative towards OM with less nitrogen species. Alternatively, during post and pre monsoon, a positive intercept is on PN (0.01 ; $R^2 = 0.97$) was indicative towards presence of OM more relative nitrogen species such as algal material (Matondkar et al., 2007). Therefore, an explanation can be made in support of the idea that organic carbon enriched in SPM of ZRE was majorly from soil and/or vegetative detritus, with spatial-specific pulses of nitrogen from algal sources. This was also evidenced by lower POC/PN ratio (av. 9.5). Delivery of fresh vascular-plant OM (usually have $\text{C/N} > 12$) into SPM was low and restricted to estuarine samples (mean $\text{POC/PN} = 11$), especially during pre and post monsoon, which might be related with re-suspension of bed sediment and mudflat. Overall, along the ZRE hydrograph, a transitional shift of POC enriched with inputs from plant and plankton/algae (freshwater and marine) were evidenced through positive correlations of salinity vs. $\delta^{13}\text{C}_{\text{POC}}$ (Figure 4; $p \leq 0.05$).

4.2 OM compositions and fate in ZRE

Predominant vegetation LULC with minimal mudflat LULC expectedly controls POC composition in the upstream region of ZRE, where $\delta^{13}\text{C}_{\text{POC}}$ was $\geq -30\text{‰}$ in all the seasons (Table 1; Figure 4 & 5). However, lower lignin phenol ($\delta \leq 1 \text{ mg } 100 \text{ mg}^{-1} \text{ POC}$) in majority of SPM was indicative towards lesser input of vascular plant OM into POC. Elevated levels of Chl *a* (representing the index of phytoplankton biomass) in upstream stations noticed during all the seasons were relative to high biological productivity and abundance of photosynthetically efficient phytoplankton, amenable to low salinity waters (Matondkar et al., 2007). Therefore, depleted $\delta^{13}\text{C}_{\text{POC}}$ in upstream were related with OM from autochthonous plankton productivity, with a fraction certainly derived

from vegetation detritus (evidenced by higher S/V ratio) those presumably decayed in soil, therefore can easily dilute by the phytoplankton biomass (Table 1). In estuarine SPM, the OM enriched with autochthonous production, indicated by higher $\delta^{13}\text{C}_{\text{POC}}$ ($\delta^{13}\text{C}_{\text{POC}}$ (21‰ to 23‰) and lower $\delta^{15}\text{N}$ (0.2–0.6 mg 100mg⁻¹POC). Mixing of vegetation detritus in estuarine region could be due to aquatic macrophytes present in mudflat and usually have enriched $\delta^{13}\text{C}_{\text{POC}}$ (25‰ to 28‰; Hunsinger et al., 2012) and low $\delta^{15}\text{N}$ (~ 0.5 mg 100mg⁻¹C_{org}; Pradhan et al., 2014).

Due to the effect of dilution by OM mixture from plankton and soil, signatures of plant OM in SPM were scattered along SPM gradient, which was indicated by negative correlations of $\delta^{15}\text{N}$ vs. salinity (-0.71, -0.90 and -0.98; $p \leq 0.01$; during SWM, post and pre-monsoon, respectively) and Pn/P vs. salinity (-0.76, -0.77 and -0.60; $p \leq 0.05$; during SWM, post and pre-monsoon, respectively). Decrease of $\delta^{15}\text{N}$ and Pn/P along with increased salinity in ZRE was indicative of disproportionate mixing of plant OM with algal materials during all seasons (Benner et al., 1990). The fraction of plant OM derived from sedimentary re-suspension owing to ETM and or mudflat LULC, especially during pre and postmonsoon cannot be ruled out in this study because C/V and (Ad/Al)_{VP} ratios decreased with increasing mudflat LULC, without any covariance with vegetation LULC, whereas the Pn/P ratio decreased with increasing vegetation cover (Table 1). The dilution process of lignin due to autochthonous phytoplankton production is obvious in large tropical aquatic systems such as Sepitiba Bay (Rezende et al., 2010) and Mekong River (Ellis et al., 2012). However, lignin dilution is complex in small river–estuary systems like ZRE, which was due to varying intensity of riverine biological, protracted ETM dynamic sand dam regulated freshwater runoff.

Faster sinking of plant OM in ZRE was evidenced through higher $\delta^{15}\text{N}$ in sediment (Table 2). The plant OM in SPM were mainly from non-woody tissues of angiosperm leaves and grasses, whereas in sediment, woody tissues contributes to significant fraction of plant OM indicative through C/V and S/V ranges, also lower LPVI (Table 2; Figure 6; Hedges and Mann, 1979; Tareq et al., 2004). The faster sinking of plant OM into sediment is due to change in vegetation LULC in the basin that provoked rapid sinking of woody plant tissues. The featured vegetation LULC showed negative interrelationship with S/V ratio, which probably highlight that change in vegetation LULC has potential linkage with presence of woody tissues in the sediment (Figure 7). The faster sinking of plant OM also enhanced deposition of fresh plant tissues in sediment as compared to the SPM, which is highlighted by lower (Ad/Al)_{VP} ratio (<0.5; describe the fresh plant tissue; Hedges and Mann, 1979). The higher (Ad/Al)_{VP} ratios in SPM could be due to lignin sorption on minerals, which often result low mass yield of lignin (e.g. Keil et al., 1997). Such process that could be linked to mining activity and/or sewage input in ZRE is unlikely, because both these sources constituted negligible

lignin phenols (Pradhan et al., 2014). One of the major processes that control rapid sinking of plant OM in estuarine environment is hydrodynamic shorting (e.g. Bianchi et al., 2007), which in case of ZRE was overwhelmed by seasonal movement of ETM, lower freshwater runoff and associated sediment re-suspension that removes fine sediment from the mudflat and transport seaward direction in ZRE (Rao et al., 2011). Therefore, the efficient transportation of plant derived OM in ZRE is largely inhibited, which also provoke the removal of degraded OM into SPM. Impact of reservoir construction on biogeochemical cycling of OM in large river systems e.g. Yangtze (Yu et al., 2011), Mekong (Ellis et al., 2012) and Congo (Spencer et al., 2010) are distinct. The downstream fate of the OM largely constrained because OM is mostly trapped behind the dam. The disproportionally varying OM signatures observed in ZRE and its interrelationship with featured LULC is likely to complicate the quantitative capacity of terrestrial OM in ocean.

4.3 Factors influencing OM characteristics in ZRE

The seasonal OM composition change in ZRE is influenced by factors such as biological production and physical mixing. Association of vegetation LULC with biological production indicated about admixture of vegetative detritus in the freshwater region, mainly degraded with lignin. Similarly, association of mudflat LULC with $\delta^{13}C$ in the mixing factor is indicative towards plant OM input due to lateral mixing (Figure 8). The quantitative as well as qualitative OM transport in ZRE is therefore affected by fluvial discharge during SWM and in situ primary production during non-monsoon periods, which could be further naturally bio available in coastal region. The effect of LULC is strong and related with compositional change of OM in ZRE, which accounts to 42%, 2% and 97% during SWM, post and pre-monsoon respectively, by vegetation LULC. Whereas, the effect accounts to 58%, 98% and 3% during SWM, post and pre-monsoon, respectively, by mudflat LULC. Briefly, the variability of allochthonous OM was regulated by physical mixing and triggered with mudflat LULC, which may largely affect the process of fluvial carbon transport. The in-situ riverine autochthonous OM modulated through vegetation LULC and brings forth changes into the seasonality of OM in ZRE. Impact of natural and/or anthropogenic processes on abundance and lability of OM is an important constrain across many tropical SMREs (Kessarkar et al., 2013; Jennerjahn et al., 2008; Moyer et al., 2013; Wu et al., 2013). Due to the short transit time from source to the Arabian Sea, the OM properties in fluvial matters within ZRE should be less altered. However, OM composition in ZRE is strongly modulated by key factors such as LULC change and damming, which hampers the seasonality.

4.4 Provenance of OM in ZRE

The ranges of $\delta^{13}\text{C}_{\text{POC}}$ (-20.7‰ to -34.1‰) and $\delta^{13}\text{C}_{\text{org}}$ (-23.4‰ to -27.3‰) highlighted OM contributions from multiple sources (freshwater plankton: -25‰ to -35‰ ; marine plankton: -18‰ to -22‰ ; C_3 plants: -21‰ to -32‰ ; soils: -23‰ to -30‰ and algal detritus: -26‰ to -30‰) in ZRE (Figure 9; Hemilton and Lewis, 1992; Barros et al., 2010; Pradhan et al., 2014). Generally, $\delta^{13}\text{C}$ signatures of soil OM is indistinguishable from the OM mixture of vascular plants and plankton, but soil OM has reasonably higher $\delta^{18}\text{O}$ than plankton. Similarly, $\delta^{18}\text{O}$ in fresh vascular plant material is much higher than soil OM; also $\delta^{13}\text{C}$ of vascular plants is lower than soil but closer to riverine plankton (Figure 9). The detritus OM, in ZRE is mainly admixture of algae, therefore constitute lower lignin phenols (Goni et al., 2003).

Due to higher freshwater productivity and close proximity of land margins, OM contributed from soil and plankton was higher in SPM of riverine region. Seasonally movable ETM and mudflat LULC contributed significantly to mixing of re-suspended soil OM into SPM in the estuarine region. The OM contribution from marine plankton into SPM of bay remained higher during all seasons. This can be attributed to the complexly functioned ETM in ZRE bay, which act as a shield that restricts the transport of marine OM landward and this instigate the removal process of soil and plankton materials through re-suspension and delivered into the channel region. However, such complexity was observed during SWM and post-monsoon throughout the bay and channel probably relevant with expansion of ETM zone, whereas the same during pre-monsoon occurred within a close proximity of bay. The sedimentary OM was characterized by soil and algal detritus owing to deposition and removal process in ZRE. The seasonal investigation of ZRE highlighted an exceptional situation of limited seasonality of biogeochemical properties, mainly conducive with physical mixing and biological productivity that are transformed by LULC, ETM and damming.

5. Conclusion

Multiple OM tracers were used to understand the fundamental linkage among LULC, hydrology and OM composition in particulate and sedimentary carbon pools of ZRE, a tropical SMRE along the western peninsular India. The information is crucial for constraining natural vs. anthropogenic activities influencing OM compositions in SMREs, also the terrestrial carbon budget of Arabian Sea. Based on the distribution of geochemical tracers over space-time scale, we draw the following conclusions:

- (i) Monsoonal freshwater discharge delayed by a month in ZRE due to dam and excess rainfall caused disproportionate water runoff through tributary. Vegetation dominated LULC declined

along the ZRE basin with increased mudflats, together have hampered seasonality of OM biogeochemistry in ZRE.

- (ii) ZRE showcased as low SPM-high Chl *a* system, with lower carbon export capacity (20×10^3 kg yr⁻¹) majorly contributed from plankton and vegetation detritus in SPM, whereas from fresh vascular plant in sediment.
- (iii) Strong interaction between LULC and OM properties, which highlighted shifting of C_{org} and $\delta^{13}C$ values from river-estuary by 20% and 60%, respectively mainly due to mudflat, nevertheless it constitutes only 3% in ZRE.
- (iv) The composition of plant OM in SPM were mainly from non-woody tissues of angiosperm leaves and grasses, whereas from woody tissues in sediment.
- (v) Autochthonous production and lateral physical mixing are two key factors controlling OM composition variation in ZRE. Additionally, the effect of vegetation LULC accounts to 42%, 2% and 97% of overall OM composition during SWM, post and pre-monsoon, respectively, whereas effects of mudflat accounts to 58%, 98% and 3% during SWM, post and pre-monsoon, respectively.

Efficient OM transport from small river-estuary systems to the Arabian Sea is largely inhibited by seasonal flow control by dam as well as LULC is an important environmental problem. The transformation, entrapment and sinking of terrestrial OM in tropical SMREs, as highlighted in this study are critical and model example of human usage of environment, nevertheless the tropical SMREs are the effective transporters of terrestrial carbon to the ocean and contributes significantly to the global carbon cycling. Effective policy aspects towards sustainable management of fluvial discharge through tropical SMREs is a need of hour in view of their capricious role towards carbon and nutrient transport into global ocean.

Acknowledgements

Authors thankful to Director, CSIR-NIO and Scientist-in-Charge CSIR-NIO, RC Mumbai for encouragement towards this study. Analytical measurements done at SKLEC (State Key laboratory of Estuarine and Coastal Research, PR China) during UKP's visit, expenses were met under NSFC (Natural Science Foundation of China) grants (41021064, 41076052), SKLEC (2010RCDW04, 2012RCDW05), 111 Project (B08022). UKP sincerely thank to MHRD (Ministry of Human Resource Development), Govt. of India and Chinese Scholarship Council, PR China for providing visiting fellowship. The authors sincerely thanks to anonymous reviewers of this MS. The article bears CSIR-NIO's contribution No. XXXX.

6. References

1. Anderson, J. R., Hardy, E. E., Roach, J. T. and Witmer, R. E. 1976. A Land Use and Land Cover Classification System for Use with Remote Sensor Data Geological Survey Professional Paper 964
2. Barros, G.V., Martinelli, L.A., Novais, T.M.O., Ometto, J.P.H. and Zuppi, G.M., 2010. Stable isotopes of bulk organic matter to trace carbon and nitrogen dynamics in an estuarine ecosystem in Babitonga Bay (Santa Catarina, Brazil). *Science of the Total Environment*, 408(10), pp.2226-2232.
3. Benner, R., Weliky, K. and Hedges, J.I., 1990. Early diagenesis of mangrove leaves in a tropical estuary: molecular-level analyses of neutral sugars and lignin-derived phenols. *Geochimica et Cosmochimica Acta*, 54(7), pp.1991-2001.
4. Bianchi, T.S., Wysocki, L.A., Stewart, M., Filley, T.R. and McKee, B.A., 2007. Temporal variability in terrestrially-derived sources of particulate organic carbon in the lower Mississippi River and its upper tributaries. *Geochimica et Cosmochimica Acta*, 71(18), pp.4425-4437.
5. Bolton, E.W., Berner, R.A. and Petsch, S.T., 2006. The weathering of sedimentary organic matter as a control on atmospheric O₂: II. Theoretical modeling. *American Journal of Science*, 306(8), pp.575-615.
6. Bouillon, S., Abril, G., Borges, A.V., Dehairs, F., Govers, G., Hughes, H., Merckx, R., Meysman, F., Nyunja, J., Osburn, C. and Middelburg, J.J., 2009. Distribution, origin and cycling of carbon in the Tana River (Kenya): a dry season basin-scale survey from headwaters to the delta. *Biogeosciences*, 6(11), pp.2475-2493.
7. Coplen, T.B., 2011. Guidelines and recommended terms for expression of stable-isotope-ratio and gas-ratio measurement results. *Rapid communications in mass spectrometry*, 25(17), pp.2538-2560.
8. Dubois, S., Savoye, N., Grémare, A., Plus, M., Charlier, K., Beltoise, A. and Blanchet, H., 2012. Origin and composition of sediment organic matter in a coastal semi-enclosed ecosystem: an elemental and isotopic study at the ecosystem space scale. *Journal of Marine Systems*, 94, pp.64-73.
9. Ellis, E.E., Keil, R.G., Ingalls, A.E., Richey, J.E. and Alin, S.R., 2012. Seasonal variability in the sources of particulate organic matter of the Mekong River as discerned by elemental and lignin analyses. *Journal of Geophysical Research: Biogeosciences*, 117(G1).
10. Gomez, B., Trustrum, N.A., Hicks, D.M., Rogers, K.M., Page, M.J. and Tate, K.R., 2003. Production, storage, and output of particulate organic carbon: Waipaoa River basin, New Zealand. *Water Resources Research*, 39(6).
11. Goñi, M.A. and Montgomery, S., 2000. Alkaline CuO oxidation with a microwave digestion system: Lignin analyses of geochemical samples. *Analytical chemistry*, 72(14), pp.3116-3121.
12. Goñi, M.A., Teixeira, M.J. and Perkey, D.W., 2003. Sources and distribution of organic matter in a river-dominated estuary (Winyah Bay, SC, USA). *Estuarine, Coastal and Shelf Science*, 57(5-6), pp.1023-1048.

13. Hedges, J.I. and Mann, D.C., 1979. The characterization of plant tissues by their lignin oxidation products. *Geochimica et Cosmochimica Acta*, 43(11), pp.1803-1807.
14. Hedges, J.I., Ertel, J.R. and Leopold, E.B., 1982. Lignin geochemistry of a Late Quaternary sediment core from Lake Washington. *Geochimica et Cosmochimica Acta*, 46(10), pp.1869-1877.
15. Hedges, J.I., Turin, H.J. and Ertel, J.R., 1984. Sources and distributions of sedimentary organic matter in the Columbia River drainage basin, Washington and Oregon 1. *Limnology and Oceanography*, 29(1), pp.35-46.
16. Hedges, J.I., Clark, W.A., Quay, P.D., Richey, J.E., Devol, A.H. and Santos, M., 1986. Compositions and fluxes of particulate organic material in the Amazon River1. *Limnology and Oceanography*, 31(4), pp.717-738.
17. Hamilton, S.K. and Lewis Jr, W.M., 1992. Stable carbon and nitrogen isotopes in algae and detritus from the Orinoco River floodplain, Venezuela. *Geochimica et Cosmochimica Acta*, 56(12), pp.4237-4246.
18. Hernes, P.J., Spencer, R.G., Dyda, R.Y., Pellerin, B.A., Bachand, P.A. and Bergamaschi, B.A., 2008. The role of hydrologic regimes on dissolved organic carbon composition in an agricultural watershed. *Geochimica et Cosmochimica Acta*, 72(21), pp.5266-5277.
19. Hilton, R.G., Galy, A., Hovius, N., Horng, M.J. and Chen, H., 2010. The isotopic composition of particulate organic carbon in mountain rivers of Taiwan. *Geochimica et Cosmochimica Acta*, 74(11), pp.3164-3181.
20. Hilton, R.G., Galy, V., Gaillardet, J., Dellinger, M., Bryant, C., O'Regan, M., Gröcke, D.R., Coxall, H., Bouchez, J. and Calmels, D., 2015. Erosion of organic carbon in the Arctic as a geological carbon dioxide sink. *Nature*, 524(7563), p.84.
21. Houel, S., Louchouart, P., Lucotte, M., Canuel, R. and Ghaleb, B., 2006. Translocation of soil organic matter following reservoir impoundment in boreal systems: Implications for in situ productivity. *Limnology and oceanography*, 51(3), pp.1497-1513.
22. Huang, T.H., Fu, Y.H., Pan, P.Y. and Chen, C.T.A., 2012. Fluvial carbon fluxes in tropical rivers. *Current Opinion in Environmental Sustainability*, 4(2), pp.162-169.
23. Hunsinger, G.B., Mitra, S., Findlay, S.E. and Fischer, D.T., 2012. Littoral-zone influences on particulate organic matter composition along the freshwater-tidal Hudson River, New York. *Limnology and Oceanography*, 57(5), pp.1303-1316.
24. Jackson, A.L., Inger, R., Bearhop, S. and Parnell, A., 2009. Erroneous behaviour of MixSIR, a recently published Bayesian isotope mixing model: a discussion of Moore & Semmens (2008). *Ecology Letters*, 12(3), pp.E1-E5.
25. Jennerjahn, T.C., Ittekkot, V., Klöpper, S., Adi, S., Nugroho, S.P., Sudiana, N., Yusmal, A. and Gaye-Haake, B., 2004. Biogeochemistry of a tropical river affected by human activities in its catchment: Brantas River estuary and coastal waters of Madura Strait, Java, Indonesia. *Estuarine, Coastal and Shelf Science*, 60(3), pp.503-514.

26. Jennerjahn, T.C., Soman, K., Ittekkot, V., Nordhaus, I., Sooraj, S., Priya, R.S. and Lahajnar, N., 2008. Effect of land use on the biogeochemistry of dissolved nutrients and suspended and sedimentary organic matter in the tropical Kallada River and Ashtamudi estuary, Kerala, India. *Biogeochemistry*, 90(1), pp.29-47.
27. Kao, S.J. and Milliman, J.D., 2008. Water and sediment discharge from small mountainous rivers, Taiwan: The roles of lithology, episodic events, and human activities. *The Journal of Geology*, 116(5), pp.431-448.
28. Keil, R.G., Mayer, L.M., Quay, P.D., Richey, J.E. and Hedges, J.I., 1997. Loss of organic matter from riverine particles in deltas. *Geochimica et Cosmochimica acta*, 61(7), pp.1507-1511.
29. Kessarkar, P.M., Shynu, R., Rao, V.P., Chong, F., Narvekar, T. and Zhang, J., 2013. Geochemistry of the suspended sediment in the estuaries of the Mandovi and Zuari rivers, central west coast of India. *Environmental monitoring and assessment*, 185(5), pp.4461-4480.
30. Khodse, V.B. and Bhosle, N.B., 2012. Nature and sources of suspended particulate organic matter in a tropical estuary during the monsoon and pre-monsoon: Insights from stable isotopes ($\delta^{13}\text{C}_{\text{POC}}$, $\delta^{15}\text{N}_{\text{TPN}}$) and carbohydrate signature compounds. *Marine Chemistry*, 145, pp.16-28.
31. Krishna, M.S., Naidu, S.A., Subbaiah, C.V., Gawade, L., Sarma, V.V.S.S. and Reddy, N.P.C., 2015. Sources, distribution and preservation of organic matter in a tropical estuary (Godavari, India). *Estuaries and coasts*, 38(3), pp.1032-1047.
32. Lloret, E., Dessert, C., Pastor, L., Lajeunesse, E., Crispi, O., Gaillardet, J. and Benedetti, M.F., 2013. Dynamic of particulate and dissolved organic carbon in small volcanic mountainous tropical watersheds. *Chemical Geology*, 351, pp.229-244.
33. Lorenzen, C.J., 1967. Determination of chlorophyll and phaeo-pigments: spectrophotometric equations 1. *Limnology and oceanography*, 12(2), pp.343-346.
34. Lyons, W.B., Nezat, C.A., Carey, A.E. and Hicks, D.M., 2002. Organic carbon fluxes to the ocean from high-standing islands. *Geology*, 30(5), pp.443-446.
35. Matondkar, S.P., Gomes, H.D., Parab, S.G., Pednekar, S. and Goes, J.I., 2007. Phytoplankton diversity, biomass and production. *The Mandovi and Zuari Estuaries. Dona Paula, Goa, India: National Institute of Oceanography*, pp.67-81.
36. Milliman, J.D. and Syvitski, J.P., 1992. Geomorphic/tectonic control of sediment discharge to the ocean: the importance of small mountainous rivers. *The journal of Geology*, 100(5), pp.525-544.
37. Milliman, J.D., Farnsworth, K.L. and Albertin, C.S., 1999. Flux and fate of fluvial sediments leaving large islands in the East Indies. *Journal of Sea Research*, 41(1-2), pp.97-107.
38. Moyer, R.P., Bauer, J.E. and Grotoli, A.G., 2013. Carbon isotope biogeochemistry of tropical small mountainous river, estuarine, and coastal systems of Puerto Rico. *Biogeochemistry*, 112(1-3), pp.589-612.

39. Nandargi, S. and Mulye, S.S., 2014. Spatio-Temporal rainfall variability and rainstorm analysis over the Goa State, India. *Studies in Atmospheric Science*, 1, pp.8-23.
40. Otto, A. and Simpson, M.J., 2005. Degradation and preservation of vascular plant-derived biomarkers in grassland and forest soils from Western Canada. *Biogeochemistry*, 74(3), pp.377-409.
41. Paimpillil, J.S. and Nair, M. 2012. Impact of iron and manganese mining activities: Arsenic in marine and wetland sediments. In: Understanding the Geological and Medical Interface of Arsenic (Eds.) J.C. Ng, B.N. Noller, R. Naidu, J. Bundschuh, P. Bhattacharya, CRC Press London, pp 433–434.
42. Panda, D.K., Kumar, A. and Mohanty, S., 2011. Recent trends in sediment load of the tropical (Peninsular) river basins of India. *Global and Planetary Change*, 75(3-4), pp.108-118.
43. Parnell, A.C., Inger, R., Bearhop, S. and Jackson, A.L., 2010. Source partitioning using stable isotopes: coping with too much variation. *PloS one*, 5(3), p.e9672.
44. Pradhan, U.K., Wu, Y., Shirodkar, P.V., Zhang, J. and Zhang, G., 2014. Sources and distribution of organic matter in thirty five tropical estuaries along the west coast of India-a preliminary assessment. *Estuarine, Coastal and Shelf Science*, 151, pp.21-33.
45. Pradhan, U.K., Wu, Y., Wang, X., Zhang, J. and Zhang, G., 2016. Signals of typhoon induced hydrologic alteration in particulate organic matter from largest tropical river system of Hainan Island, South China Sea. *Journal of hydrology*, 534, pp.553-566.
46. Ramaiah, N., Rodrigues, V., Alwares, E., Rodrigues, C., Baksh, R., Jayan, S. and Mohandass, C., 2007. *The Mandovi and Zuari Estuaries. Dona Paula, Goa, India: National Institute of Oceanography*, pp.115-120.
47. Rao, V.P., Shynu, R., Kessarkar, P.M., Sundar, D., Michael, G.S., Narvekar, T., Blossom, V. and Mehra, P., 2011. Suspended sediment dynamics on a seasonal scale in the Mandovi and Zuari estuaries, central west coast of India. *Estuarine, Coastal and Shelf Science*, 91(1), pp.78-86.
48. Reddy, B.S.R. and Rao, V.R., 1994. Seasonal variation in temperature and salinity in the Gautami-Godavari estuary. *Proceedings of the Indian Academy of Sciences-Earth and Planetary Sciences*, 103(1), pp.47-55.
49. Rezende, C.E., Pfeiffer, W.C., Martinelli, L.A., Tsamakis, E., Hedges, J.I. and Keil, R.G., 2010. Lignin phenols used to infer organic matter sources to Sepetiba Bay–RJ, Brasil. *Estuarine, Coastal and Shelf Science*, 87(3), pp.479-486.
50. Sarkar, A., Chakraborty, P. and Nath, B.N., 2016. Distribution and nature of sedimentary organic matter in a tropical estuary: An indicator of human intervention on environment. *Marine pollution bulletin*, 102(1), pp.176-186.
51. Sarma, V.V.S.S., Viswanadham, R., Rao, G.D., Prasad, V.R., Kumar, B.S.K., Naidu, S.A., Kumar, N.A., Rao, D.B., Sridevi, T., Krishna, M.S. and Reddy, N.P.C., 2012. Carbon dioxide emissions from Indian monsoonal estuaries. *Geophysical Research Letters*, 39(3).

52. Prakash, S., Sathiyamoorthy, V., Mahesh, C. and Gairola, R.M., 2013. Is summer monsoon rainfall over the west coast of India decreasing?. *Atmospheric Science Letters*, 14(3), pp.160-163.
53. Spencer, R.G., Hernes, P.J., Ruf, R., Baker, A., Dyda, R.Y., Stubbins, A. and Six, J., 2010. Temporal controls on dissolved organic matter and lignin biogeochemistry in a pristine tropical river, Democratic Republic of Congo. *Journal of Geophysical Research: Biogeosciences*, 115(G3).
54. Sundar, D. and Shetye, S.R., 2005. Tides in the Mandovi and Zuari estuaries, Goa, west coast of India. *Journal of Earth System Science*, 114(5), pp.493-503.
55. Sundar, D., Unnikrishnan, A.S., Michael, G.S., Kankonkar, A., Nidheesh, A.G. and Subeesh, M.P., 2015. Observed variations in stratification and currents in the Zuari estuary, west coast of India. *Environmental Earth Sciences*, 74(9), pp.6951-6965.
56. Tareq, S.M., Tanaka, N. and Ohta, K., 2004. Biomarker signature in tropical wetland: lignin phenol vegetation index (LPVI) and its implications for reconstructing the paleoenvironment. *Science of the Total Environment*, 324(1-3), pp.91-103.
57. Wafar, S., Untawale, A.G. and Wafar, M., 1997. Litter fall and energy flux in a mangrove ecosystem. *Estuarine, Coastal and Shelf Science*, 44(1), pp.111-124.
58. Watson, J.G., Zhu, T., Chow, J.C., Engelbrecht, J., Fujita, E.M. and Wilson, W.E., 2002. Receptor modeling application framework for particle source apportionment. *Chemosphere*, 49(9), pp.1093-1136.
59. Wohl, E., Dwire, K., Sutfin, N., Polvi, L. and Bazan, R., 2012. Mechanisms of carbon storage in mountainous headwater rivers. *Nature communications*, 3, p.1263.
60. Wu, Y., Bao, H.Y., Unger, D., Herbeck, L.S., Zhu, Z.Y., Zhang, J. and Jennerjahn, T.C., 2013. Biogeochemical behavior of organic carbon in a small tropical river and estuary, Hainan, China. *Continental Shelf Research*, 57, pp.32-43.
61. Yu, H., Wu, Y., Zhang, J., Deng, B. and Zhu, Z., 2011. Impact of extreme drought and the Three Gorges Dam on transport of particulate terrestrial organic carbon in the Changjiang (Yangtze) River. *Journal of Geophysical Research: Earth Surface*, 116(F4).
62. Zhang, J., Wang, D.R., Jennerjahn, T. and Dsikowitzky, L., 2013. Land–sea interactions at the east coast of Hainan Island, South China Sea: a synthesis. *Continental Shelf Research*, 57, pp.132-142.

Figure captions:

Figure 1: Upper panel: River network of Goa, with Zuari River Estuary (ZRE) shaded in light grey. Arrow marks in the estuary are direction of freshwater outflow (solid) and coastal water inflow (dashed). Lower panel: Featured land-use/Land-cover (LULC) over ZRE during (a) pre and (b) post damming periods along with sampling points. Source: (<http://earthexplorer.usgs.gov/>).

Figure 2: Mean monthly rainfall relative to annual rainfall over South Goa (Source: www.imd.gov.in). Grey bars represent proportional contribution of individual month to the annual rainfall during study period. Dashed line represents 100-year average (Source: Nandargi et al., 2014 and personal communication).

Figure 3: (a) Mean monthly freshwater flow of tributaries during 2011 and 1978 in ZRE (Data source of before construction of selaulim dam: Shetye et al., 2007). (b) Mean monthly freshwater flow ratios between Kushavati and upper tributaries during this study as well as before damming. (c) Changes in average monthly water flow between 2011 and 1978. SWM refers to southwest monsoon.

Figure 4: Seasonal variation of geochemical parameters along the salinity gradient of ZRE. Significant variations of parameters are displayed through regression lines and R^2 values.

Figure 5: Spatial variation in geochemical parameters and ratios in line with featured LULC (vegetation, agriculture and mudflat) areas computed from 5 km² box area proximal to the sampling stations (presented in Table 1).

Figure 6: Property-property plot of C/V and S/V ratios. The proximal limits of C/V and S/V of SPM (hollow symbol) and sediment (solid symbol) plotted along with the literature end-member limits (blue solid diamonds) to highlight the composition of plant tissues present in samples from ZRE. (Source: Goñi et al., 2003; Rezende et al., 2010; Pradhan et al., 2014)

Figure 7: Interrelationship between geochemical parameters and featured LULC along the longitudinal gradient of ZRE.

Figure 8: Principal component analysis depicting association of geochemical parameters along with LULC on different factor plane during different seasons in ZRE.

Figure 9: Seasonal contribution of OM from different sources to the SPM and sediment from ZRE. End member limits adopted from Hedges et al., 1986; Rezende et al., 2010; Pradhan et al., 2014.

Table captions

Table 1: Panel A: Spatial pattern of LULC within 5 km × 5 km grid around the sampling stations over ZRE and basin wide LULC during pre-damming (1976) and present (2015). Abbreviated LULC categories are; CL: Cultivable land, SC: Settlement with mixed crop, FP: Forest with plantation, MG: Mangrove, MN: Mining, OS: open scrubland and WB: Water bodies and their area of coverage in km². Panel B: Hydrographic characteristics, elemental contents, bulk isotopic and lignin phenol characteristics in particulate samples from all sampling sites during different seasons in ZRE. Statistical significance of parameters varied among different seasons highlighted through p-values obtained by single factor ANOVA and the $p \leq 0.05$ (bold) represent 95% of significance in the analysis.

Table 2: Elemental contents, bulk isotopic and lignin phenol characteristics in carbon end-members (plant and soils) as well as sediment samples collected during different seasons in ZRE.

Table 1: Panel A

Area under LULC categories (km²)	CL	SC	FP	MG	MN	MF	OS	WB
<i>Spatial variability in LULC during 2015</i>								
Z6	0.3	0.3	0.2	–	–	0	0	19.6
Z5	–	1.8	0.2	0.1	–	0.1	1.0	17.1
Z4	3.1	3.9	2.8	1.2	–	3.9	1.4	4.0
Z3	2.7	4.1	6.9	0.2	–	3.0	1.0	2.4
Z2	2.1	4.5	11.9	1.2	–	0	0.2	0.3
Z1	2.0	2.7	14.1	–	–	0	1.4	0.1
<i>Long term LULC variability in ZRE</i>								
1976 (Pre-damming)	292.4	12	505.3	0.6	1.2	21.6	140.6	25.8
2015 (Present)	113.2	117.2	638.3	11.7	6.7	31.1	44.3	37

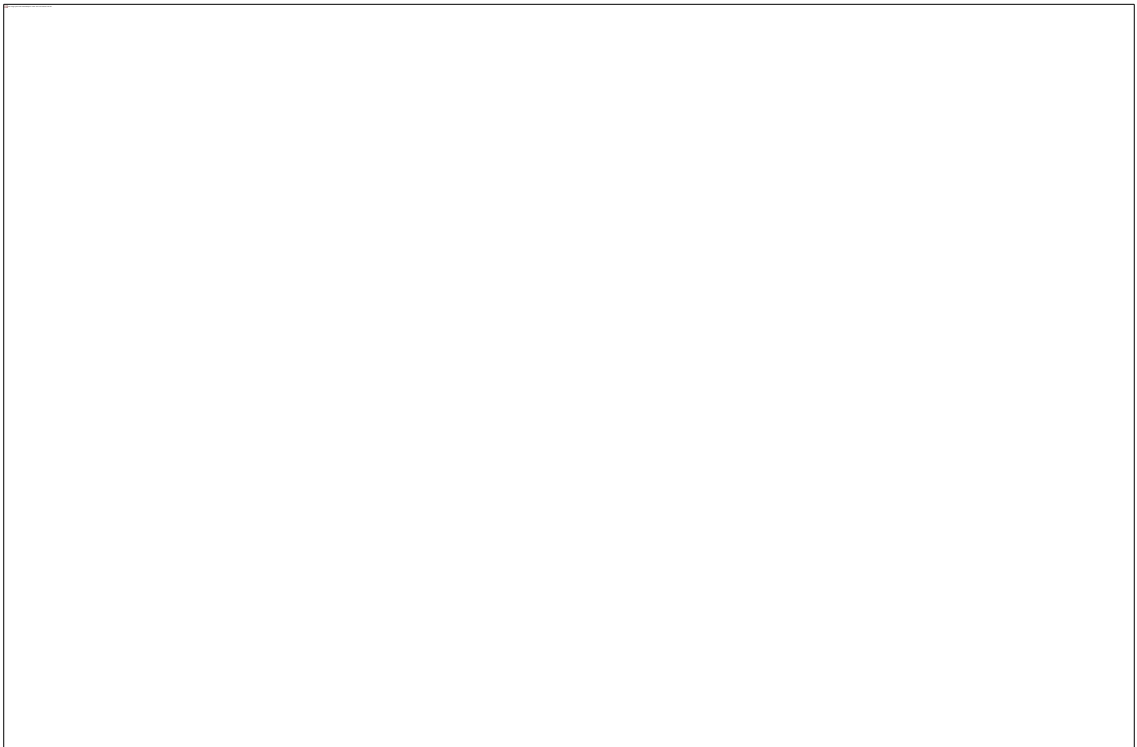
Panel B

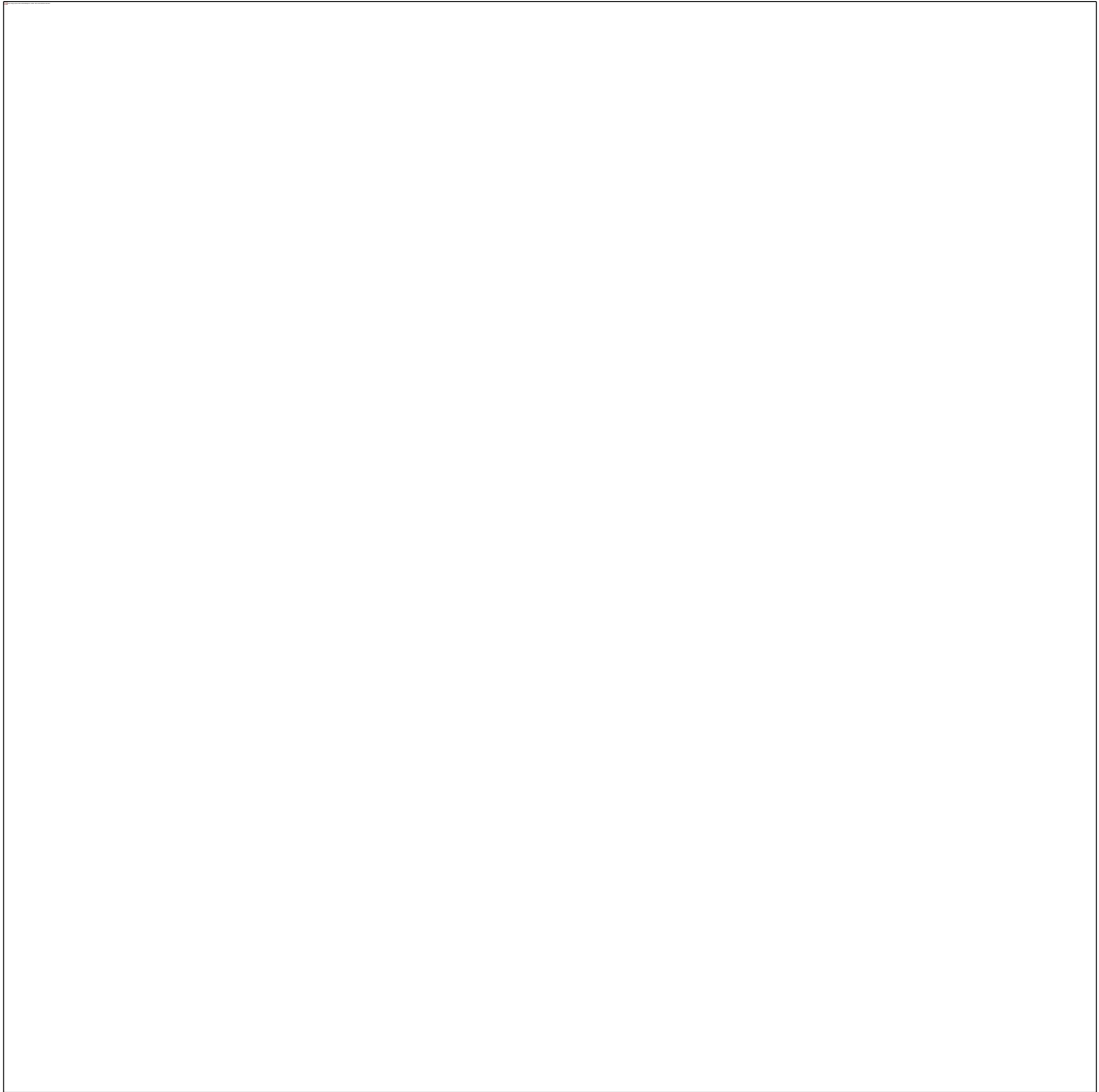
Stations	Temp. (°C)	pH	Salinity (psu)	SPM (mgL ⁻¹)	Chl-a (mg g ⁻¹)	POC (%)	δ ¹³ C _{POC} (‰)	POC/PN	δ ⁸ mg100 mg ⁻¹ POC)	δ ⁸ (mg10g ⁻¹)	Lignin (%CuO)	(Ad/Al) _v	DHBA/V	Pn/P	LPVI
<i>South west monsoon (SWM)</i>															
Z6	29.4	8.1	18.9	13.6	1.4	3.32	-22.8	9.8	0.23	0.78	13.2	0.79	0.24	0.02	500
Z5	29.3	8.1	18.4	33.0	1.2	2.01	-22.1	7.9	0.21	0.61	20.7	1.22	0.26	0.04	159
Z4	29.2	7.5	7.5	10.9	1.2	3.21	-28.4	7.8	0.47	1.52	33.6	1.59	0.22	0.07	216
Z3	28.0	7.0	0.0	9.7	1.1	8.48	-28.5	1.6	0.94	7.97	48.0	1.06	0.10	0.07	98
Z1	29.2	6.6	0.0	1.3	0.5	38.8	-34.1	17.0	0.71	27.5	27.5	3.33	0.41	0.05	314
<i>Post-monsoon</i>															
Z6	30.4	8.2	33.7	17.3	0.7	1.57	-20.7	6.6	0.32	0.60	26.6	1.15	0.15	0.05	571
Z5	30.5	8.1	33.7	18.5	1.2	1.55	-21.0	9.1	0.60	0.93	25.7	1.54	0.18	0.04	428
Z4	31.1	8.0	31.1	44.4	0.3	1.40	-23.0	10.1	1.89	2.65	68.3	0.73	0.10	0.08	136
Z3	30.6	7.0	10.4	27.3	0.6	2.76	-27.3	11.7	1.14	3.15	54.2	0.84	0.12	0.08	216
Z2	29.1	6.9	0.0	11.0	0.9	9.36	-29.4	11.7	0.68	6.37	26.6	0.96	0.12	0.09	307
<i>Pre-monsoon</i>															
Z5	31.0	8.1	35.0	18.9	0.6	1.82	-21.7	9.0	0.21	0.40	22.6	0.89	0.13	0.04	131
Z4	31.3	7.9	32.2	165.6	0.1	2.06	-23.4	11.7	0.25	0.52	31.5	0.59	0.15	0.03	183
Z3	33.0	7.6	17.6	22.1	1.0	3.56	-29.6	7.7	0.47	1.68	30.9	0.59	0.15	0.03	171
Z2	33.0	7.2	0.0	8.3	1.3	11.7	-31.5	8.0	0.43	5.03	34.4	0.85	0.18	0.04	290
Z1	32.3	7.0	0.0	3.5	1.0	13.4	-33.6	8.1	0.38	5.13	23.8	0.92	0.16	0.06	159
<i>p-value</i>	0.01	0.76	0.02	0.41	0.38	0.44	0.12	0.33	0.13	0.15	0.09	0.54	0.03	0.04	0.35

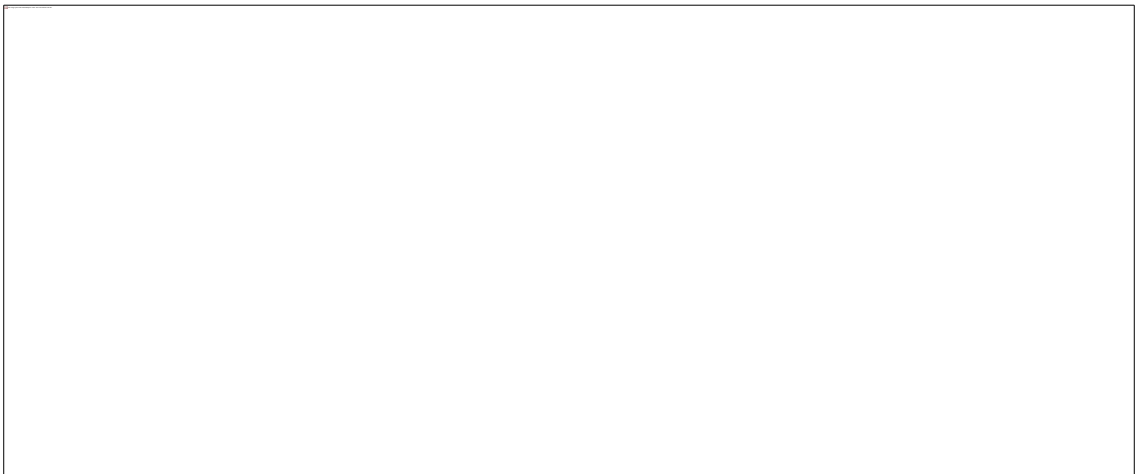
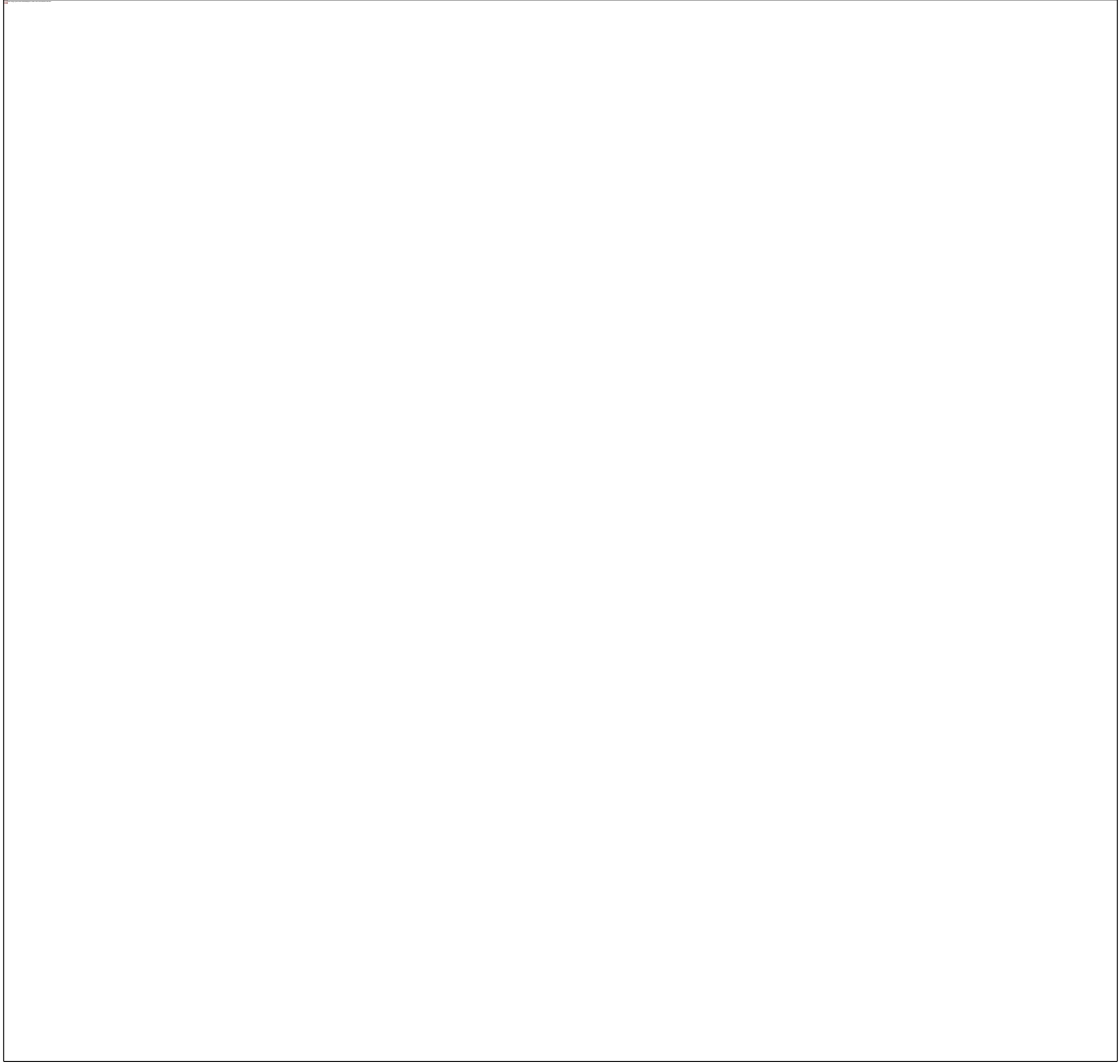
Table 2:

Sample	C _{org} (wt. %)	TN (wt. %)	C _{org} /N	□ ¹³ C _{org} (‰)	□8(mg100 mg ⁻¹ C _{org})	□8 (mg 10g ⁻¹ dry wt.)	(Ad/Al) _v	Lignin (%SVC)	LPVI	Clay (%)	Silt (%)	Sand (%)
Botanical sample												
K. candel (<i>leaf</i>)	34.70	2.54	13.6	-30.4	2.56	88.8	0.46	85.2	1799			
S. alba (<i>leaf</i>)	37.60	1.72	21.9	-28.3	2.76	103.9	0.36	75.8	574			
A. officinalis (<i>leaf</i>)	36.00	2.98	12.1	-30.0	4.71	169.5	0.44	92.0	1747			
R. mucronata (<i>leaf</i>)	40.20	1.53	26.3	-27.7	2.77	111.6	0.68	62.5	2409			
S. Caseolaris (<i>leaf</i>)	38.60	1.94	19.9	-26.6	7.57	292.1	0.45	63.2	52			
Oryza sativa (<i>leaf</i>)	31.00	1.71	18.1	-29.5	5.76	178.6	0.29	85.7	2525			
Tectona grandis (<i>leaf</i>)	32.50	0.52	62.7	-28.3	3.80	123.4	0.55	73.3	69			
Artocarpus heterophyllus (<i>leaf</i>)	38.90	0.42	91.7	-29.8	10.08	391.9	0.26	91.6	268			
A. Marina (<i>wood</i>)	45.62	0.99	46.0	-30.3	7.77	323.9	0.26	92.7	101			
A. officinalis (<i>wood</i>)	43.30	1.05	41.1	-29.3	5.93	256.1	0.24	82.9	247			
Tectona grandis (<i>wood</i>)	41.11	0.41	99.2	-29.9	3.83	157.4	0.33	61.4	406			
S. caseolaris (<i>flower</i>)	35.98	2.74	13.1	-24.3	3.26	117.3	0.50	48.3	22			
Calendula Officinalis (<i>flower</i>)	45.69	2.04	22.4	–	1.60	72.9	0.28	62.8	540			
chrysanthemum (<i>flower</i>)	44.00	2.01	21.8	–	2.19	96.3	0.71	40.0	163			
Rose (<i>flower</i>)	45.73	2.30	19.9	–	0.97	44.3	0.19	25.1	23			
Soils												
Soil (<i>mine-tailings</i>)	0.09	0.01	19.4	-22.1	1.22	0.1	0.26	67.5	102	–	–	–
Soil (<i>mine-tailings</i>)	0.08	<0.01	25.9	-22.9	0.86	0.1	0.15	53.4	10	–	–	–
Soil(<i>mountainous</i>)	0.65	0.06	12.9	-21.4	0.18	0.1	0.59	80.6	79	–	–	–
Bottom sediments												
Z5 (<i>SWM</i>)	0.59	0.05	11.5	-23.8	1.64	1.0	0.49	86.3	46	12.0	34.0	54.0
Z4 (<i>SWM</i>)	2.56	0.20	12.7	-25.1	5.96	15.5	0.32	93.0	44	30.4	43.0	26.7
Z3 (<i>SWM</i>)	1.12	0.10	10.7	-26.5	3.08	3.4	0.48	85.5	95	19.8	34.6	45.5
Z1 (<i>SWM</i>)	1.21	0.11	10.6	-26.0	1.62	1.9	0.44	80.3	15	26.1	57.3	16.6
Z6 (<i>post-monsoon</i>)	0.71	0.03	22.9	-23.6	0.64	0.2	0.46	79.4	77	19.3	45.6	35.2
Z3 (<i>post-monsoon</i>)	2.45	0.23	10.5	-25.3	3.30	8.3	0.29	87.0	119	37.1	51.5	11.4
Z2 (<i>post-monsoon</i>)	2.74	0.23	12.0	-27.3	3.99	10.8	0.26	88.0	185	27.1	53.6	19.3
Z5 (<i>pre-monsoon</i>)	2.70	0.05	50.8	-25.7	4.34	11.7	0.30	90.3	66	35.5	54.9	9.5
Z4 (<i>pre-monsoon</i>)	0.61	0.25	2.5	-23.8	1.15	0.7	0.42	85.5	42	2.5	3.6	93.9
Z3 (<i>pre-monsoon</i>)	2.35	0.23	10.2	-24.8	2.93	6.7	0.35	87.7	61	39.5	51.9	8.7

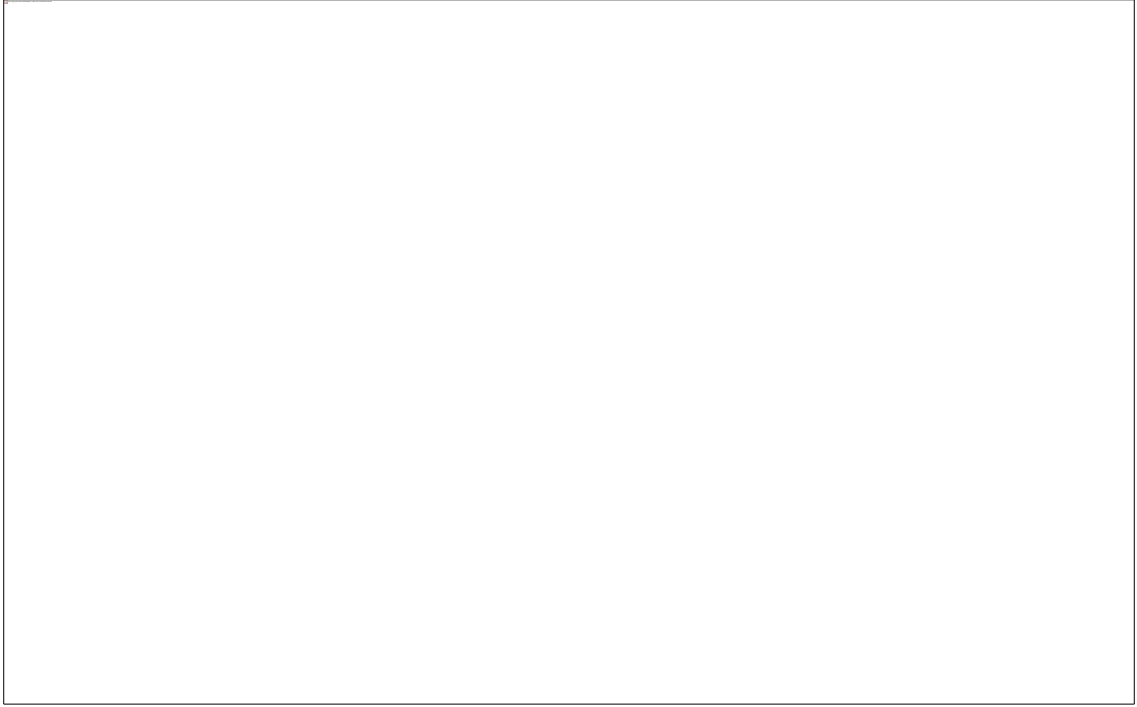
1

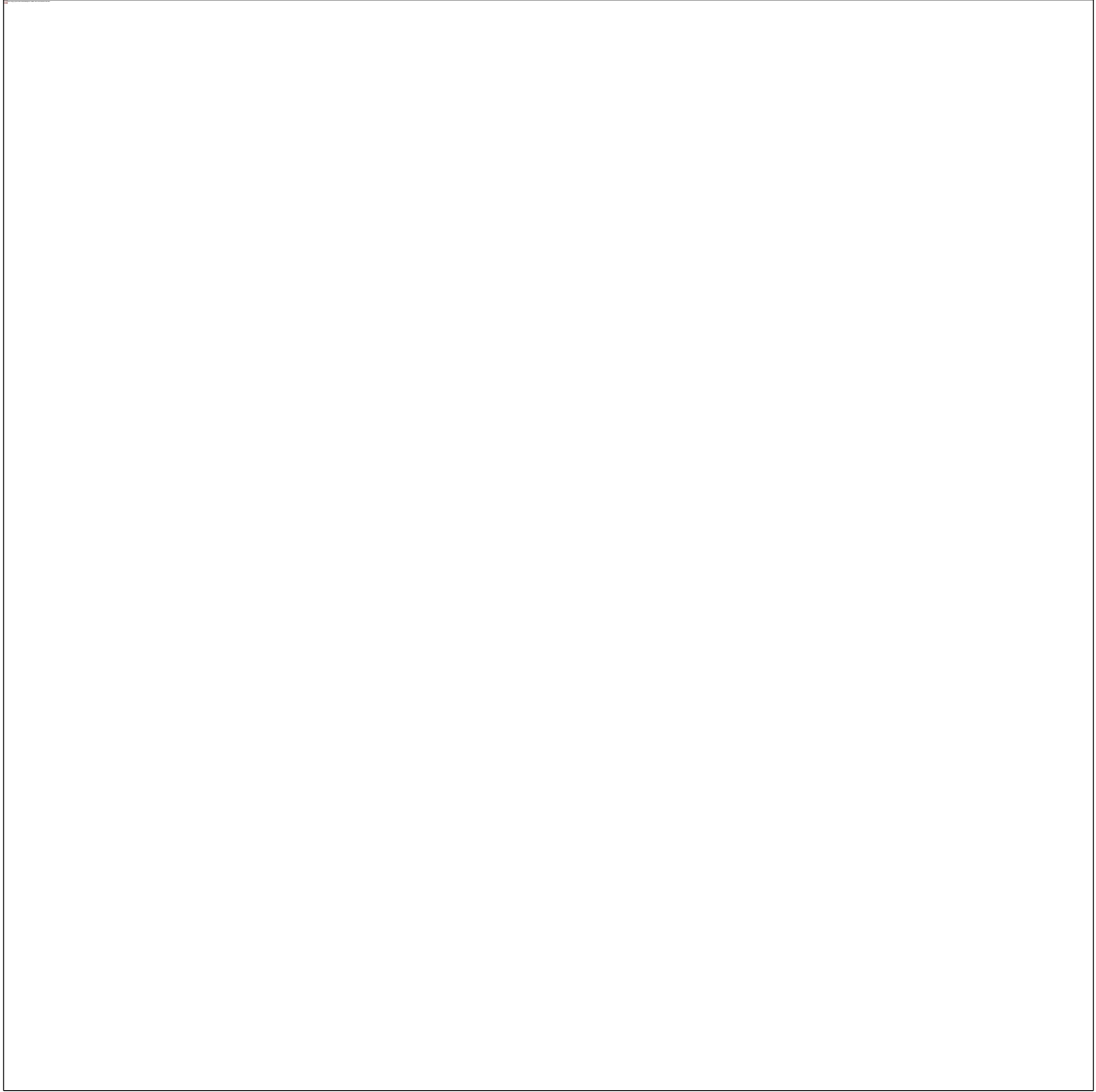












Supplementary Table: Distribution of relative abundance of CuO oxidation products. SPM have higher abundance of P(non-lignin) phenols and sediments have higher lignin phenols.

SPM	Pl (%)	Pn (%)	Pd (%)	Vl (%)	Vn (%)	Vd (%)	Sl (%)	Sn (%)	Sd (%)	PCD (%)	FAD (%)	DHBA (%)	SVC (%)	P (%)
<i>SWM</i>														
Z6	60.1	1.9	23.8	2.1	1.0	1.7	1.5	3.5	1.0	1.0	1.2	1.2	13.0	85.8
Z5	44.4	3.1	29.8	3.4	2.2	4.1	1.9	4.0	2.1	1.3	1.4	2.5	20.2	77.3
Z4	35.2	4.2	24.8	4.4	3.6	7.0	2.9	5.2	4.4	2.6	2.5	3.3	32.5	64.1
Z3	33.6	3.3	13.8	9.4	5.5	9.9	5.6	6.0	4.6	3.6	2.2	2.6	46.8	50.6
Z1	41.3	3.5	24.1	2.0	3.0	6.8	1.4	4.0	2.1	3.0	3.7	4.9	26.1	69.0
<i>Post monsoon</i>														
Z6	47.6	3.8	20.9	3.4	2.7	3.9	2.3	6.0	2.5	2.3	3.1	1.5	26.2	72.3
Z5	45.4	3.0	24.5	2.7	2.9	4.2	2.3	6.5	2.4	1.9	2.2	1.7	25.3	73.0
Z4	18.4	2.4	9.9	13.9	7.0	10.1	10.4	9.4	8.6	3.0	3.7	3.2	66.1	30.7
Z3	21.7	3.0	15.0	10.7	6.2	9.0	7.2	8.7	6.9	4.3	4.2	3.2	57.1	39.7
Z2	22.9	3.9	17.8	8.9	5.2	8.5	4.7	9.7	6.5	4.7	4.5	2.7	52.7	44.6
<i>Pre monsoon</i>														
Z5	55.9	2.8	17.6	4.5	2.6	4.1	2.2	3.9	1.9	1.0	2.0	1.5	22.2	76.3
Z4	51.9	2.2	13.0	7.2	2.9	4.3	4.7	4.5	2.9	1.6	2.7	2.1	30.8	67.1
Z3	52.3	2.3	13.1	7.1	3.0	4.1	4.9	4.6	2.7	1.6	2.3	2.1	30.3	67.6
Z2	46.2	2.6	15.1	6.1	3.4	5.2	3.5	5.7	3.7	2.9	3.0	2.6	33.5	63.9
Z1	51.3	4.2	19.4	4.4	2.4	4.0	3.0	4.1	2.8	1.6	1.1	1.7	23.4	74.9
Sediment	Pl (%)	Pn (%)	Pd (%)	Vl (%)	Vn (%)	Vd (%)	Sl (%)	Sn (%)	Sd (%)	PCD (%)	FAD (%)	DHBA (%)	SVC (%)	P (%)
<i>SWM</i>														
Z5	5.6	1.5	5.9	24.1	8.3	11.8	18.5	7.0	8.1	2.1	1.5	5.7	81.4	12.9
Z4	2.9	0.9	3.1	30.8	8.6	9.8	22.7	8.0	7.7	1.4	1.8	2.4	90.7	6.9
Z3	6.0	1.7	5.9	20.9	7.1	10.0	20.0	7.8	8.8	3.1	2.4	6.2	80.2	13.6
Z1	9.7	1.9	6.6	29.4	9.8	12.9	9.3	4.3	4.3	2.7	1.6	7.4	74.4	18.2
<i>Post- monsoon</i>														
Z6	8.2	1.9	9.1	20.2	7.3	9.3	19.0	7.4	5.9	2.4	2.3	7.0	73.9	19.1
Z3	5.1	1.4	6.1	25.4	6.9	7.5	23.0	7.6	6.1	3.6	4.0	3.2	84.1	12.6
Z2	4.4	1.4	5.8	25.2	6.5	6.6	22.5	8.4	6.1	5.5	4.6	2.9	85.5	11.6
<i>Pre- monsoon</i>														
Z5	5.8	1.8	6.2	25.2	8.4	10.5	19.8	8.1	6.8	1.4	1.1	5.0	81.2	13.8
Z4	4.2	1.2	4.1	27.6	7.9	8.4	23.3	7.9	7.3	2.2	2.5	3.6	87.1	9.4
Z3	5.1	1.5	4.9	24.8	7.9	8.6	23.1	8.5	6.8	1.9	1.4	5.5	82.9	11.6